# Flexibility as a Model Parachute Performance Parameter

H. G. HEINRICH* AND THOMAS R. HEKTNER†
*University of Minnesota, Minneapolis, Minn.*

**In parachute model experiments, performed for the study of static and dynamic parachute characteristics, one must consider, besides Reynolds and Mach number influences, the effects of canopy porosity, weight, and flexibility. Porosity can be expressed as a function of Reynolds and Mach numbers. For the definition of the structural characteristics, a stiffness-weight index is proposed. Fabrication details for building models with a low stiffness index were developed. Wind-tunnel and catapult tests with models of different stiffness indexes showed significant differences in parachute drag, inflation, and squidding characteristics.**

## Nomenclature

$C$ = effective porosity
$C_D$ = drag coefficient
$C_T$ = tangent force coefficient
$d$ = diameter of lower strip curvature
$D$ = diameter
$D_{\max}$ = maximum width of the suspended strip specimens of model canopies
$D_{\max}/L$ = strip stiffness index
$D_{p\max}$ = maximum projected diameter of the inflated parachute
$E_p$ = canopy skirt elongation
$F$ = force
$g$ = gravity
$L$ = length of strip specimens
$m$ = mass [included mass $m_i = \frac{1}{12}(\rho\pi D_p^3)$]
$S$ = area
$T$ = dimensionless filling time, $t/t_f$
$t$ = time
$v$ = velocity
$W$ = weight; width of strip specimens
$w_{cl}$ = weight of cloth per unit area
$\alpha$ = angle of attack
$\rho$ = density
$\eta$ = canopy stiffness index, $(D_{\max}/L)\cdot(W_c/S_0w_{cl})$
$\gamma$ = angle of suspension line cone or angle of ribbon handles of strips

### *Subscripts*

$a$ = apparent
$c$ = canopy
$cl$ = cloth
eff = effective
$f$ = filling
$i$ = included, inlet
0 = nominal, total
$p$ = parachute, projected
$s$ = suspended, snatch when used with velocity
$st$ = stable or trim when used with $\alpha$
$w$ = wind tunnel

## I. Introduction

AERODYNAMIC and dynamic performance characteristics of ballistic and lifting bodies can be predicted satisfactorily from model test data when conventional model similarity laws are obeyed. Influential similarity conditions for steady-state aerodynamic measurements are the Mach and Reynolds numbers and, for low density, the Knudsen number. For aeroelastic deformations and nonsteady aerodynamic phenomena, more sophisticated model laws must be applied.[1]

Under proper similarity conditions, model test results are valid for prediction of performance characteristics over a wide range of environmental conditions. For example, for the Apollo capsule, aerodynamic data obtained with models having a diameter of but 0.95 cm agree perfectly with data obtained from Apollo missions.[2]

Contrary to this experience is the fact that performance data of parachutes in wind-tunnel tests differ in many cases considerably from full-size drop test data. This discrepancy has been recorded in steady-state as well as in nonsteady parachute processes. Considering first discrepancies in steady-state performance, such as the rate of descent, and assuming that parachute models and prototypes have been tested under suitable Mach and Reynolds number conditions and that the test data have been properly evaluated, the question arises as to the accuracy of the full-size test recordings. Valid recordings are difficult to obtain because of unknown currents, possibly varying glide angles, and dynamic stability phenomena. However, in cases where results from many carefully conducted field tests are available and discrepancies still exist, one must admit that the reasons for them are unknown.

Efforts to predict parachute inflation characteristics on the basis of model tests date back to 1941.[3] However, still lacking is a satisfactory method of calculating opening forces based on model test results or on direct comparison of forces obtained from model and full-size tests.

In the search for reasons for these difficulties, one notices that parachutes have at least two features not commonly found in conventional airborne vehicle aerodynamics, namely, porosity and flexibility.

In the steady-state condition, the probability of a varying deformation or pulsation of the parachute canopy is relatively small. This phase is thus primarily governed by steady-state aerodynamic coefficients and parachute size. The coefficients are influenced by parachute material porosity.[4] The relationship between coefficients and porosity, as well as the dependency of porosity upon Mach and Reynolds numbers, is fairly well understood.[5] However, even with careful consideration of these influences, the results of parachute model and full-size tests under steady-state conditions still disagree. Therefore, it is justified to investigate a possible relationship between model flexibility and inflated size.

The nonsteady performance phases encompass dynamic stability and the inflation process. The dynamic stability characteristics depend on the aerodynamic coefficients and the shape and deformation of the canopy profile under oscil-

Presented as Paper 70-1166 at the AIAA Aerodynamic Deceleration Systems Conference, Dayton, Ohio, September 14–16, 1970; submitted September 15, 1970; revision received March 29, 1971. This study was sponsored by U.S. Air Force Contract F33615-68-C-1227.

Index Categories: Aircraft Deceleration Systems; Post-Entry Deceleration Systems and Flight Mechanics; Re-Entry Vehicle Testing.

* Professor. Fellow AIAA.
† Associate Scientist.

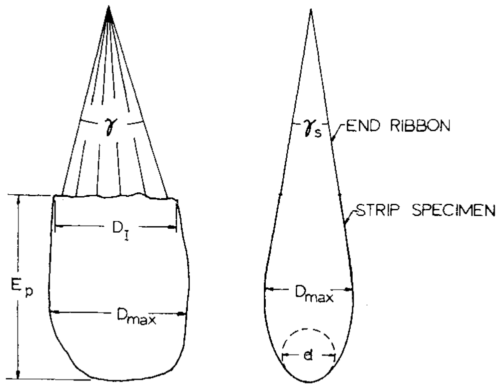


**Fig. 1 Parachute canopy suspension test characteristics.**

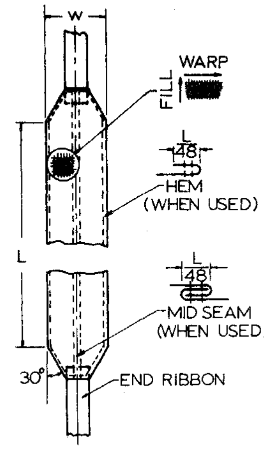


**Fig. 2 Strip fabrication details.**

lation. Otherwise, the problems of dynamic stability are well understood.[6]

In the nonsteady phase of inflation, a parachute canopy evolves from the form of an elongated sack to that of a thin semiellipsoidal shell. The inflation process is governed by the balance of the mass in- and outfluxes, which, in turn, depend upon effective canopy porosity. As stated previously, the relationship between porosity and Mach and Reynolds numbers is known[5] and can be introduced in the equations that govern the opening process. However, it is possible that model and full-size parachutes tend to open faster or slower, depending on their inherent stiffness. If model tests show that stiffness characteristics significantly influence opening, then the prediction of the opening characteristics, on the basis of model tests, must also include consideration of canopy flexibility.

## II. Stiffness Index

Unfortunately, no publication on the subject of parachute stiffness has been found. Therefore, an original attempt was made to express the degree of canopy stiffness or flexibility in quantitative terms. Figure 1 shows a characterization of a freely suspended parachute and elementary strip contours. Using the ratio of $D_{max}$ to $D_0$ as a characteristic parameter, one finds $D_{max}/D_0 = 0.09$ and 0.29 for a 28-ft prototype parachute and a conventionally built 5-ft parachute model, respectively. This indicates that the prototype parachute is much more flexible than the geometrically similar model built of the same cloth. Measurements with other models provided essentially the same results.

The parachute cloth cannot be modified because the material porosity features must be preserved, and it is probably beyond the state of the art to weave "model cloth." However, it should be possible to build more flexible models by using different types of seams, more flexible suspension lines, and new methods of suspension line fastening. Therefore, attention was directed toward the elements that compose the parachute canopy, and this led to the study of stiffness of model strips, also shown in Fig. 1.

The ratio of $D_{max}$ to strip length again reflects its stiffness or flexibility and will, for the time being, be called stiffness index. Figure 2 shows fabrication details for a particular model strip.

A number of strips with different seams and various suspension lines and line attachments were investigated, and the results as well as the seam arrangement scheme are shown in Fig. 3. Strips without seams at the edges have the lowest stiffness index, and, furthermore, strips cut with a heated sharp edge (so-called hot knife) are at least as flexible as strips cut with a conventional pair of scissors. Cutting with a hot knife provides seared edges on the strip which prevent the material from fraying. In these strip tests, possibly existing charges of static electricity were removed by humidifying the surrounding air.

One may assume that parachute canopies built on the principles of the most flexible strips will provide models with low stiffness indexes. Most parachute models now used were made somewhat similar to full-size parachutes, which, in the 5-ft model size, gives stiffness indexes at least four times higher than the related prototype. In view of the strip test results, the hot-knife-cut technique was used in the fabrication of new model canopies. Also, a new method was developed to fasten the thin, very flexible suspension lines. In this method, shown in Fig. 4, the suspension lines are anchored at the vent and the skirt and can slide over the canopy cloth in a manner somewhat similar to the suspension lines of full-size parachutes. Also, the model has a seared edge instead of a skirt seam or band. This technique has also been used to fabricate ringslot canopies.

Parachute models, as described previously, were more flexible and much lighter than conventionally built models. Because, during the inflation, the enclosed air primarily accelerates the material of the canopy radially, canopy weight is also important. Therefore, a weight term was introduced into the canopy stiffness index in the form of the ratio of the weight per unit area of the ready-made canopy to the canopy cloth unit weight. The parachute canopy stiffness index then assumes the form

$$\eta = (D_{max}/D_0) \cdot [W_c/(S_0 \cdot w_{cl})]$$

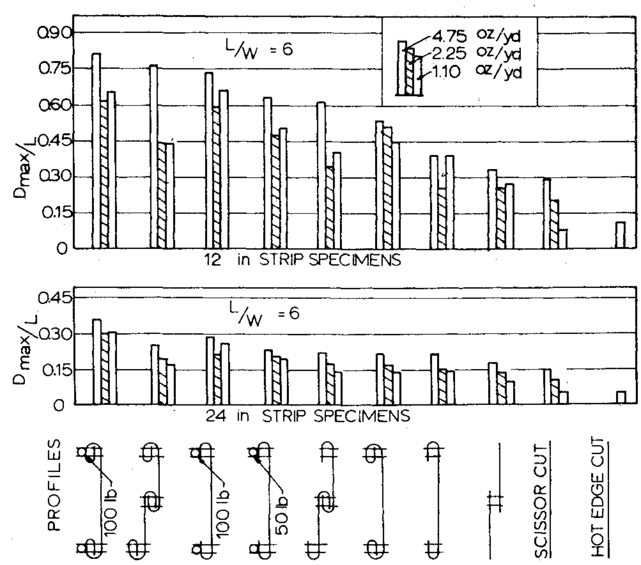


**Fig. 3 Stiffness indexes of geometrically similar 12- and 24-in. strips of different nylon materials.**

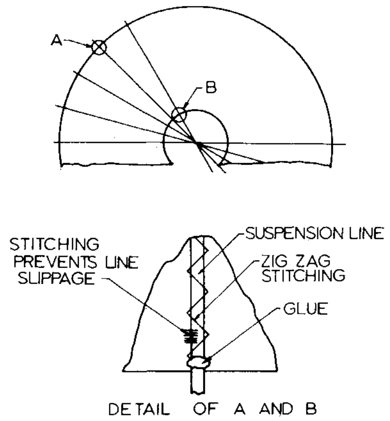


**Fig. 4 Flexible solid flat parachute construction details.**

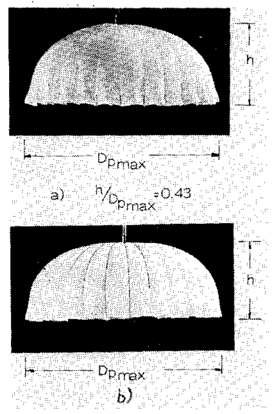


**Fig. 6 a) Conventional and b) flexible models of a 28-gore solid flat parachute ($D_0$ = 36 in.) at 50-fps air velocity.**

This stiffness-weight parameter shall, for convenience, be called the stiffness index. Figure 5 shows stiffness indexes of flexible and conventional models of the prototype parachute, together with the range covered by the data obtained from the strip tests. One notices that the stiffness index of the most flexible model parachute is still approximately 1.65 times that of the prototype.

Since for dynamic testing a certain canopy strength is required and no further weight savings or better fabrication methods were conceived, the most flexible parachute models of Fig. 5 are considered to be the current end result of these efforts.

## III. Effect of Model Stiffness

After parachute models with lower stiffness indexes became available, studies were made in which performance characteristics of conventional and new, more flexible models were established and could be compared with each other and, when possible, also compared with recordings obtained from full-size tests. Comparisons were made of drag, inflation, opening force, and parachute squidding characteristics.

### A. Shape and Drag Studies

Comparative views of solid flat circular, conventional, and flexible models are shown in Fig. 6. As seen, the depth-to-diameter ratio of the two models varies noticeably. Also, in other tests with different size solid flat and ringslot parachutes, the more flexible models were always more flat than the corresponding stiffer models. An evaluation of projected areas at zero angle of attack showed that the frontal area of the parachute model with the lower stiffness index was, on the average, 8% larger than the one of the stiffer model.

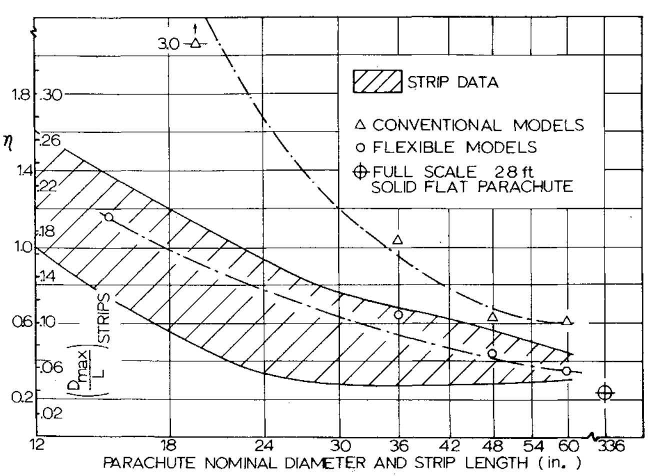


**Fig. 5 Stiffness index comparison of suspended model solid flat parachutes and strip specimens.**

Following these experiments, comparative but tentative force measurements of conventional and flexible models showed that the tangential force, at the approximate trim angle of 20° of the two models, was, on the average, 8% higher for the flexible model than for the stiffer model.

Related field tests were made by the U.S. Army Natick Laboratories with 100-ft flat circular solid cloth parachute.[7] These tests, carefully observed, indicated an average value of $C_{D_{eff}} = 0.90$ with minimum and maximum values of 0.86 and 0.93. In Ref. 4, the coefficients of flat circular parachutes were established as functions of effective porosity by means of conventionally built, relatively stiff parachute models. The results of these tests are reconsidered below in view of the newly detected flexibility influences and then compared with field-test results.

The 100-ft parachutes were made from standard parachute cloth, MIL-C-7020, type II, which specifies a nominal porosity of 130 ± 30 ft³/ft²/min at a differential pressure of $\frac{1}{2}$ in. of water (= 2.60 psf). The actual parachute descends with less differential pressure. Consequently, the effective porosity during the actual parachute descent is less than that which corresponds to the nominal porosity. Assuming that this difference amounts to 10%, one can first determine, from Ref. 4, the trim angles and the related tangent force coefficients. These amount to $C_T$ = 0.88, 0.84, and 0.79, respectively, for the effective porosities that correspond to the nominal porosities of 100, 130, and 160 ft³/ft²/min. After correcting the values of 8% in view of the area increase caused by the flexibility effect, the coefficients of effective drag[8] are 0.86, 0.905, and 0.94, which is in good agreement with the field tests. Reynolds numbers of the model and full-size tests were $4.2 \times 10^5$ and $1.7 \times 10^7$, respectively.

### B. Area- and Velocity-Time Histories during Model Parachute Inflation

Important terms in the equation of motion for parachute inflation are the instantaneous values and the time derivatives of projected and inlet areas, canopy volume, and velocity. The influence of canopy stiffness upon inflation, if it exists, must be noticeable in these quantities. Therefore, wind-tunnel experiments under finite mass conditions[4,9,10] were made with conventionally built and highly flexible models to detect possible differences.

For the wind-tunnel tests under finite mass condition, the equation of motion of the suspended mass[10] is

$$m_s\, dv/dt = \rho/[2C_D S(v_w - v)^2] - W_s + (v_w - v)\cdot[dm_i/dt + dm_a/dt] - (m_p + m_i + m_a)\, dv/dt$$

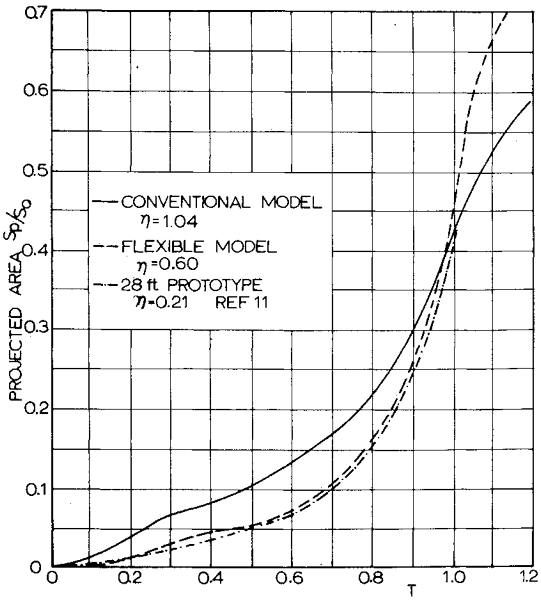


**Fig. 7 Area-time history of a conventional model ($\eta$ = 1.04) and a flexible model ($\eta$ = 0.60) at 50-fps snatch velocity.**

In Ref. 10, it was shown that drag, velocity, and mass strongly influence the force acting on the suspended weight. Therefore, experiments were made in which average values of the important time functions were established. Figure 7 shows typical area-time curves for a flexible model obtained in this manner, as well as the same characteristics for a prototype and a stiffer parachute model. Tests at different velocities were made, and in all cases the rate of growth of the projected area of the more flexible models was smaller in the early phase of inflation than the one of conventional models. In the final phase, the so-called overinflation of the more flexible model was considerably higher than that of the stiffer model. The projected area of the parachute models under steady-state conditions,[11] which is related to the instant $T = 1$, was measured in the wind tunnel at a wind velocity of approximately 50 fps and was 3.0 and 3.25 ft$^2$ for the conventional and flexible models, respectively.

As shown in Fig. 7, the area growth of the full-size parachute, reported by Berndt[11] and Berndt and DeWeese,[12] is less than that of the most flexible model parachute. This lower rate of growth of the prototype parachute, with its low stiffness index, fits the concept that more flexible parachutes have a slower rate of area increase.

In summary, these measurements indicate that parachute stiffness index significantly influences the slope of the area-time function.

Related to the projected area is, of course, the volume-time relationship. Its dependency upon flexibility was not established in this study, but it is obvious that the stiff and flexible models will have different volume-time functions.

Other important terms in the equation of motion are the velocity-time functions. These were obtained for flexible and stiff models by means of the same experimental arrangement. Numerous tests and averaging of the data gave the characteristic velocity-time relationships, one of which is

**Table 1 Maximum opening forces of parachute models with different stiffness indexes**

| $V_s$, fps | $(g_{\text{flex}}/g_{\text{conv}})_{T=1}$ |
|---|---|
| 50 | 0.70 |
| 70 | 0.61 |
| 85 | 0.67 |

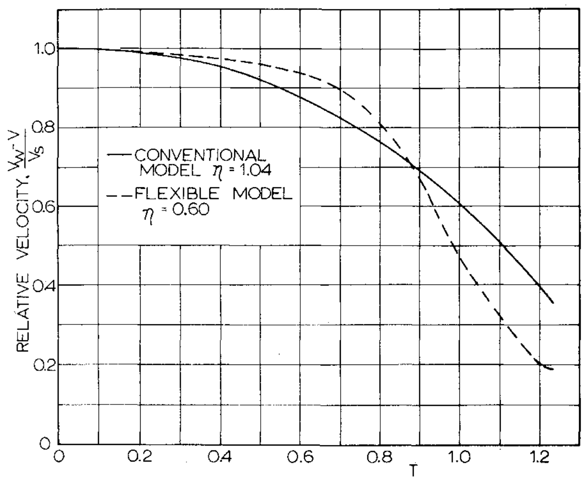


**Fig. 8 Velocity-time histories of a conventional model ($\eta$ = 1.04) and a flexible model ($\eta$ = 0.60) at 50-fps snatch velocity.**

shown in Fig. 8. In all cases, the velocity $v$ of the system of the stiffer model increased initially faster and then slower than the one of the more flexible models, which observation corresponds to the faster area growth of the stiffer models.

## C. Force-Time Histories

In view of the difference of the contributing functions in the equation of motion, one would expect canopy flexibility to influence opening forces strongly. By means of the finite mass test arrangement, numerous force-time recordings were made, and the average values of these results are presented in Fig. 9 and Table 1. In each case, the maximum opening force of the stiffer models was 30–40% higher than the corresponding force of the more flexible models.

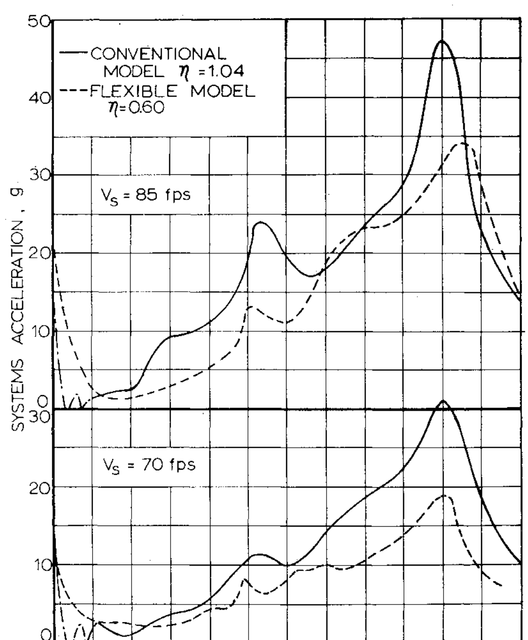


**Fig. 9 Comparison of system acceleration using conventional and flexible 3-ft model parachutes at 50, 70, and 85 fps; suspended weight = 0.5 lb.**

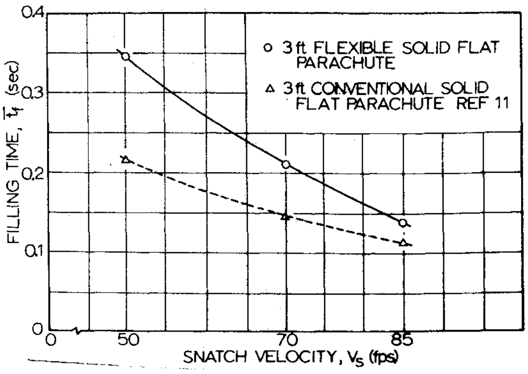


**Fig. 10 Average filling time, wind-tunnel experiments, 3-ft conventional and flexible parachute models, snatch velocities of 50, 70, and 85 fps.**

All graphs concerning the inflation process are related to the dimensionless filling time, $T = t/t_f$. The instant $T = 1$, at which the parachute canopy reaches for the first time the same projected area as it will assume at the steady-state descent[11], is of particular interest. The interval from $T = 0$ to $T = 1$ is usually called filling time $t_f$. Figure 10 shows the average filling times obtained with the conventional and the flexible parachute models. As expected, this characteristic time differs considerably for the two parachutes.

## IV. Parachute Squidding Studies

Another, but so far insufficiently explained, parachute performance characteristic is the so-called squidding. Usually squidding occurs if the surface loading of the parachute or the effective porosity is too high, and sometimes in cases of relatively high release velocities. Some field tests also have indicated that parachute stiffness influences squidding characteristics. In view of these facts, free-flight model tests were made in which the two parachute models were injected into calm air by means of a catapult. Between the parachute canopy and suspended weight, strain-gage force sensors were arranged to obtain force-time recordings during deployment, inflation, and descent. Also, the descending parachute models were photographed with a high-speed motion-picture camera.

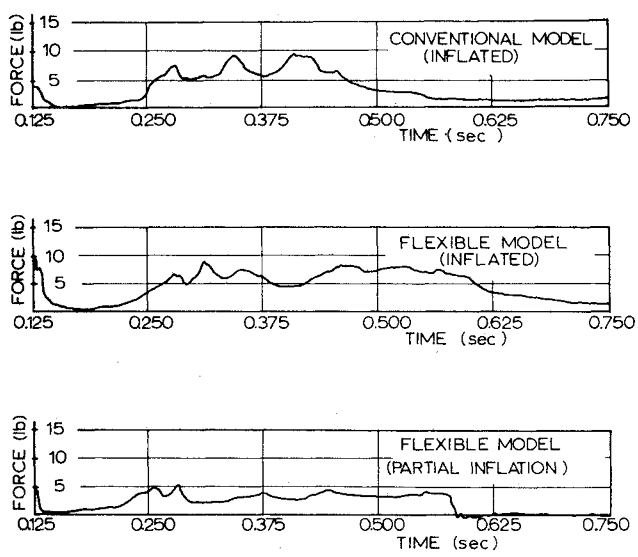


**Fig. 11 Opening force-time histories of 5-ft model parachutes, catapult test, suspended weight = 1.14 lb, $m_i/m_s$ = 0.75, snatch velocity = 50 fps.**

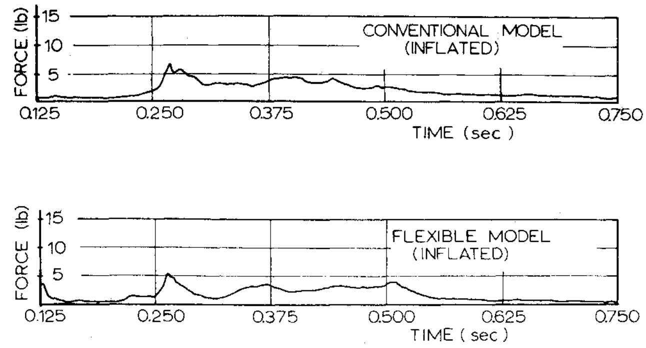


**Fig. 12 Opening force-time histories of 4-ft model parachutes, catapult test, suspended weight = 0.6 lb, $m_i/m_s$ = 0.75, snatch velocity = 50 fps.**

These tests were made to see if the often-observed squidding phenomenon could be reproduced in model tests and to find possible relationships between squidding and stiffness.

Figures 11 and 12 show force recordings taken during free flights. Referring to Fig. 11, under given test conditions, the conventional model, $\eta = 1.04$, inflated regularly and relatively quickly, whereas the flexible model, $\eta = 0.60$, failed several times to inflate fully prior to ground impact. The flexible model had the characteristic appearance of a squidding parachute. Related to these observations, the three diagrams of Fig. 11 show that the flexible parachute, when it inflated, had a lower but longer force-time history. Also, when the parachute model with the lower stiffness index failed to inflate, the sensor indicated a relatively low force prior to ground impact followed by an abrupt force reduction to zero. The time scale also indicates that the average speed of the squidding parachute was much higher than in the cases when the same parachute did inflate. Obviously, flexibility influenced the squidding characteristics.

Figure 12 shows force-time recordings of the same two types of parachutes. In these tests, the ratio of the included to suspended masses and the initial velocity was the same as before. The surface loading, however, was reduced from 0.058 to 0.048 psf. Under these conditions, both models inflated regularly, but the force-time histories differ characteristically in that 1) during inflation, the stiffer models have high peak and high average forces that act over a relatively short period of time, and 2) with all flexible models, the average as well as the peak forces were lower, but their time of action was longer. Other but less pronounced differences appear in the diagrams.

For the two flexible models, the stiffness index of the 4-ft model was approximately 22% higher than the one of the 5-ft model. Since, however, the surface loading was also decreased, it cannot conclusively be stated whether the change of surface loading, the higher stiffness index, or both caused the improvement in model performance. However, the effect of the stiffness index is noticeable in the diagrams. A further investigation of this problem would require a separate and more sophisticated study. It can, however, be stated that the model with the lower stiffness index displayed squidding, whereas the model with higher stiffness index inflated regularly, and that the influence of the stiffness index can be seen in all force recordings.

## V. Summary and Conclusion

The results of this study indicate a moderate influence of model stiffness index upon the coefficient of effective drag, a strong influence upon opening forces, and a noticeable effect upon parachute squidding characteristics.

Therefore, without consideration of the stiffness index, the drag and inflation characteristics of model parachutes are not necessarily a suitable basis for the prediction of performance characteristics of full-size parachutes.

More details about this entire field of interest are given in Ref. 13.

## References

[1] Bisplinghoff, R. L., Ashley, H., and Halfman, R. L., *Aeroelasticity*, Addison-Wesley, Cambridge, Mass., 1955.

[2] DeRose, C. E., "Thin Altitude Lift and Drag of the Apollo Command Module with Offset Center of Gravity Positions," TN 5276, 1969, NASA.

[3] Scheubel, F. N., "Der Entfaltungsvorgang des Fallschirmes (The Opening Process of Parachutes)," Deutsche Akademie der Luftfahrtsforschung (translation), 1941.

[4] Heinrich, H. G. and Haak, E. L., "Stability and Drag of Parachutes with Varying Effective Porosity," ASD-TDR-62-100, Dec. 1961, Air Force Systems Command, Wright-Patterson Air Force Base, Ohio.

[5] Heinrich, H. G., "The Effective Porosity of Parachute Cloth," *Zeitschrift fuer Flugwissenschaften 11*, Oct. 1963, pp. 389–397.

[6] White, F. M. and Wolf, D F , "A Theory of Three-Dimensional Parachute Dynamic Stability," *Journal of Aircraft*, Vol. 5, No. 1, Jan.–Feb., 1968, pp. 86–92.

[7] Shute, S. J., Jr., "The Design and Test of a Parachute to be Used in Cluster to Airdrop 50,000 Lbs," Lecture, Summer Course, Aerodynamic Deceleration '69," July 1969, Univ. of Minnesota, Airdrop Engineering Lab., U. S. Army Natick Labs., Natick, Mass.

[8] Heinrich, H. G., "Drag and Stability of Parachutes," *Aeronautical Engineering Review*, June 1956, pp. 73–81.

[9] Pounder, E., "Parachute Inflation Process Wind Tunnel Study," TR 56-391, Sept. 1956, Wright Air Development Center, Wright-Patterson Air Force Base, Ohio.

[10] Heinrich, H. G. and Noreen, R. A., "Analysis of Parachute Opening Dynamics with Supporting Wind Tunnel Experiments," *Journal of Aircraft*, Vol. 7, No. 4, July-Aug., 1970, pp. 341–347.

[11] Berndt, R. J., "Experimental Determination of Parameters for the Calculation of Parachute Filling Times," *Jahrbuch der Wissenschaftlichen Gesellschaft für Luft- und Raumfahrt E. V. (WGLR)*, 1964, pp. 299–316.

[12] Berndt, R. J. and DeWeese, H. J., "Filling Time Prediction Approach for Solid Cloth Type Parachute Canopies," *AIAA Aerodynamic Deceleration Systems Conference*, Sept. 1966, AIAA, New York, p. 454.

[13] Heinrich, H. G. and Hektner, T. R., "Flexibility as Parameters of Model Parachute Performance Characteristics," AFFDL-TR-70-53, May 1970, Air Force Systems Command, Wright-Patterson Air Force Base, Ohio.